

A SEMI-ANALYTICAL/NUMERICAL METHOD FOR PREDICTING GROUND VIBRATIONS INDUCED BY HIGH-SPEED TRAINS

Yanmei CAO*¹, He XIA¹, Fuxing WANG¹

¹School of Civil Engineering, Beijing Jiaotong University, Beijing, China, 100044
ymcao@bjtu.edu.cn

Keywords: Ground vibrations, High-speed trains, Semi-analytical train-track model, Finite/infinite subsoil model.

Abstract. *The environmental vibrations induced by high-speed railway trains have been paid more and more attention in recent years. The paper develops a method based on a semi-analytical/numerical model to predict the ground vibrations induced by high-speed trains running on ground. First, the ground vibration induced by moving loads is solved by establishing the 3-dimensional finite element soil model with infinite element boundary. The dynamic characteristics of the subsoil are analysed by applying a moving unit-harmonic-load at different speeds, and both the probable resonant frequencies of ground vibrations and the critical speed of moving loads are studied. Second, the semi-analytical train-track model is established to obtain the reaction forces on the subsoil surface, in which the vibrations of vehicle components, the quasi-static axle loads and the dynamic excitations between the wheels and track are taken into account. Then, the reaction forces on the subsoil at different train speeds are applied onto the surface of the 3-dimensional subsoil model and the ground vibrations induced by high-speed train can be obtained. The analysed results show that: the ground vibration characteristics have a very close relationship with the soil properties and the speed of moving loads; the critical speed of soil vibration is close to the minimum speed of the Rayleigh's wave in the subsoil, and the resonant frequency is very close to the intersection frequency of the speed-lines of moving loads and the P-SV dispersion curves of the subsoil model; the dynamic responses excited by wheel-track irregularity cannot be neglected, which has big influence on the high frequency components of ground vibration.*

1 INTRODUCTION

The environmental vibrations induced by high-speed railway trains have been paid more and more attention in recent years. Madshus and Kaynia [1] observed large amplitudes of displacement when the train ran on the track at high speed towards its critical speed of about 180 km/h at the measurement site. Along with their measurements, Kaynia et al [2] reported the development of a FEM model composed of a moving load on a railway embankment. Lombaert and Degrande [3] evaluated the contributions of quasi-static excitation related to the axle loads and the dynamic excitation of random track unevenness to the track and free-field responses. Sheng et al [4] modeled the ground as a structure of three-dimensional viscoelastic layers overlying either a half-space or a rigid foundation, and the track as a rail beam, a rail pad and a sleeper mass supported by a viscoelastic ballast layer. Yang [5] established a 2.5D finite/infinite element approach to study the transmissibility of soils for vibrations induced by moving trains. Auersch [6] presented a comprehensive model to analyze the ground vibration, using a combined FEM/BEM model for soil and track and a multi-DOF model for the vehicle. Takemiya [7] proposed a 2.5D FE model considering the irregular topographies of the track. Masafumi et al [8] adopted a 3D viscoelastic staggered-grid finite difference method with fourth-order accuracy in space to study the mechanism of ground vibrations induced by a high-speed train.

The paper develops a semi-analytical/numerical model to predict the ground vibrations induced by high-speed trains running on ground, and some characteristics of ground vibration are analysed by an example.

2 THERE-DIMENSIONAL FINITE/INFINITE SUBSOIL MODEL

The soil parameters adopted herein are listed in Table 1. For the dynamic characteristics of subsoil can be reflected by its cutoff frequencies, the first three cut-off frequencies of P-SV waves are calculated, and they are respectively 24.57 Hz, 43.99 Hz and 81.78 Hz. In addition, the Rayleigh wave speed of top-layer soil is 151 m/s.

Layer	Depth /m	Density /(kg/m ³)	Elastic Modulus /MPa	Poison ratio	Damping ratio
1	3.0	1350	95.59	0.37	0.05
Half-space	—	1898	506.97	0.48	0.05

Table 1: Parameters of layered half-space soil.

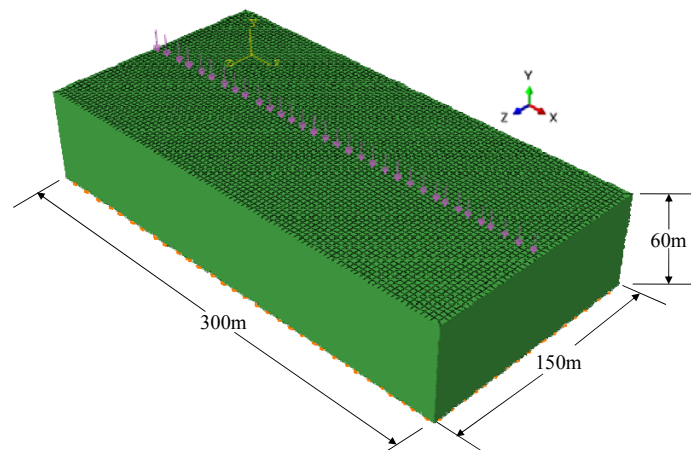


Figure 1: Three-dimensional finite/infinite subsoil model.

Figure 1 illustrates the 3-dimensional finite/infinite layered subsoil model simulated by the software of ABAQUS, in which the finite element is adopted in nearer field, the infinite elements are used in the boundary field, and they are coupled on the interface. The soil is simulated by elastic-lastic solid element, and the strain-stress relationship accords with Mohr-Coulomb yield criterion.

3 GROUND VIBRATION INDUCED BY MOVING UNIT-HARMONIC-LOAD

In order to study the influence of moving speed and soil properties on ground vibration, the ground vibrations induced by a unit-harmonic-load moving respectively at the speed of 100 m/s, 151 m/s, 200 m/s, 250 m/s, 280 m/s are studied.

Since the first-order and the second-order cutoff frequencies of the subsoil are respectively 24.57 Hz and 43.99 Hz, the vibration frequency 35 Hz in this range for the unit-harmonic-load is selected to well observe the intersection frequencies. The speed-lines of moving harmonic-loads and the P-SV dispersion curves of the subsoil model are plotted in Figure 2, in which the speed-lines of moving harmonic-loads are determined by $k=2\pi|f-f_0|/V$, thus one can find two groups of speed-lines starting from the loading frequency $f_0=35$ Hz. It can be observed from Figure 2 that the intersection frequencies of the dispersive curve of 1st order P-SV and the speed-lines of 100 m/s, 151 m/s, 200 m/s, 250 m/s and 280 m/s are respectively: 24.67 Hz (101 Hz), 211.72 Hz, 19.59Hz, 17.89Hz, 16.91Hz.

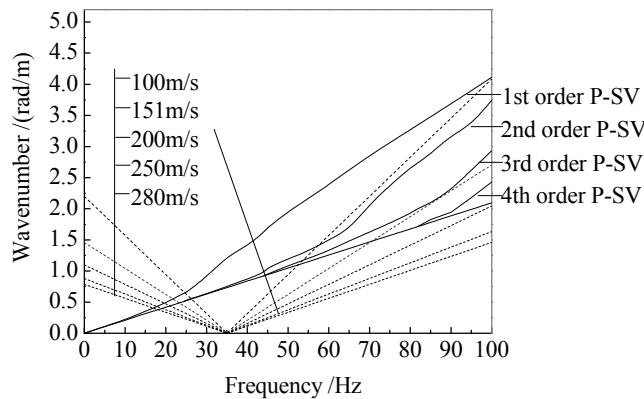


Figure 2: Distribution of P-SV dispersion curves with harmonic-load speed-lines.

By means of 3-dimensional finite/infinite subsoil model, the vertical ground displacement induced by the moving unit-harmonic-loads can be numerically calculated. Figures 3-4 show the ground displacements at a moment when the load moves at the speed of 150 m/s and 200m/s, respectively, which reflects the wave propagation with moving load.

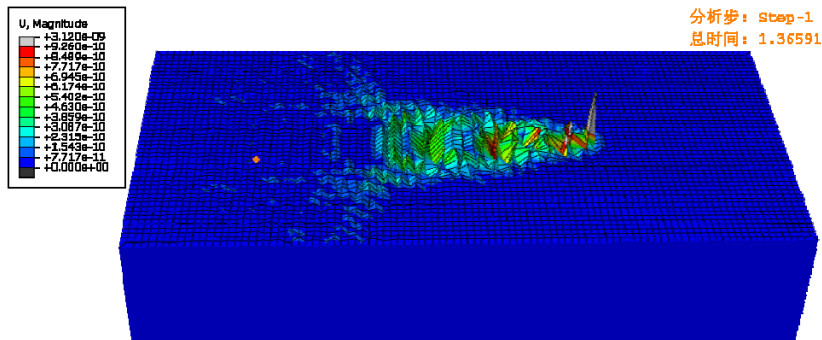


Figure 3: Ground displacement at a moment induced by moving unit-harmonic-load ($V=150$ m/s).

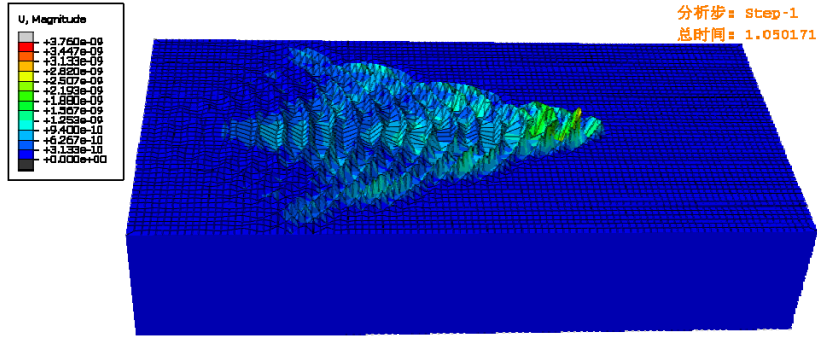


Figure 4: Ground displacement at a moment induced by moving unit-harmonic-load ($V=200\text{m/s}$).

By comparison of Figure 3 and Figure 4, it can be seen that when the moving speed is very close to the speed of Rayleigh wave of top-layer soil (151 m/s herein), the ground displacement has greater fluctuation; the greater is the moving speed of load, the wider the influence area on ground is, and the slower the wave attenuation is.

The spectra of ground displacement ($y=0\text{ m}$ and $y=8\text{ m}$) induced by moving harmonic-load are plotted in Figure 5. It can be found that the frequencies corresponding to displacement peaks are close to the intersection frequencies showed in Figure 2, which shows that the appearance of ground vibration amplification is at the resonance frequency of the soil and the moving loads. The frequencies of ground vibration induced by harmonic-loads are within a certain range, and the higher the moving speed is, the wider the frequency range is. These observations are in accordance with the results of Lombaert [9] that the frequency of ground vibration induced by moving harmonic-loads mainly concentrates on the range of $[\omega_0/(1+V/c), \omega_0/(1-V/c)]$, in which ω_0 is the vibration frequency of harmonic-load (35 Hz herein), V is the moving speed, and c is the Rayleigh's wave speed of top-layer.

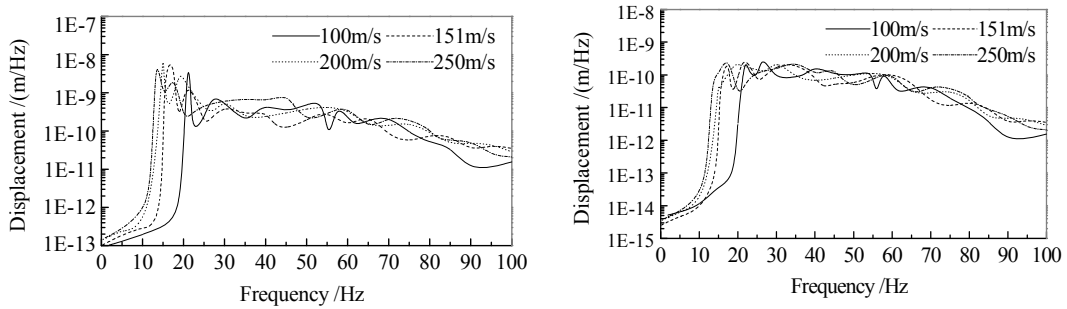


Figure 5: Spectra of ground displacement induced by moving harmonic-load: $y=0\text{ m}$ (left) and $y=8\text{ m}$ (right).

4 SEMI-ANALYTICAL TRAIN-TRACK MODEL

4.1 Train Model

The train is composed of several locomotives and passenger, and each vehicle is a multiple-DOF vibration system consisting of a car-body, bogies, wheel-sets, and spring-damper suspension system. The train-track interaction model is shown in Figure 6.

According to Lagrange motion equations, the dynamic equation of the i -th vehicle can be written as:

$$\mathbf{M}_i \ddot{\mathbf{Z}}_i + \mathbf{C}_i \dot{\mathbf{Z}}_i + \mathbf{K}_i \mathbf{Z}_i = \mathbf{P}_i(t) \quad (i=1, 2, \dots, N_v) \quad (1)$$

in which k_t and k_w are the stiffness of springs on bogie and on axle box, respectively; c_t and c_w are the damping coefficients of bogies and axle box; b is half of the distance between adjacent vehicles and a is that between adjacent bogies.

$\mathbf{P}_i(t)$ is the excitation vector acting to the i -th vehicle, which can be expressed as:

$$\mathbf{P}_i(t) = \{0 \ 0 \ 0 \ 0 \ 0 \ 0 \ -P_{i1}^{w/r}(t) \ -P_{i2}^{w/r}(t) \ \cdots \ -P_{iN_{wi}}^{w/r}(t)\}^T \quad (6)$$

in which $P_{ij}^{w/r}(t)$ represents the wheel-rail interaction force due to track irregularity of the ij -th wheel-set (short for the j -th wheel-set of i -th vehicle).

In order to study the frequency characteristics of environmental vibrations, the Fourier integral transform is carried out to Eq. (1), and the problem can be transformed from the time domain to the frequency domain as:

$$(-\mathbf{M}_i\omega^2 + i\mathbf{C}_i\omega + \mathbf{K}_i)\bar{\mathbf{Z}}_i(\omega) = \bar{\mathbf{P}}_i(\omega) \quad (7)$$

where the excitation vector can be written as $\bar{\mathbf{P}}_i(\omega) = -\mathbf{D}\bar{\mathbf{P}}_i^{w/r}(\omega)$, in which $\mathbf{D} = \begin{bmatrix} \mathbf{0}_{6 \times 4} \\ \mathbf{I}_{4 \times 4} \end{bmatrix}$ is the factor matrix of vehicle load with \mathbf{I} being unit matrix. Thus, the displacement of vehicle can be expressed as:

$$\bar{\mathbf{Z}}_i(\omega) = -(\mathbf{K}_i - \mathbf{M}_i\omega^2 + i\mathbf{C}_i\omega)^{-1}\mathbf{D}\bar{\mathbf{P}}_i^{w/r}(\omega) \quad (8)$$

If the displacement vector of wheel-sets of the i -th vehicle are denoted by $\bar{\mathbf{z}}_{wi}(\omega)$, then it can be derived to the following expression:

$$\bar{\mathbf{z}}_{wi}(\omega) = -\mathbf{D}^T(\mathbf{K}_i - \mathbf{M}_i\omega^2 + i\mathbf{C}_i\omega)^{-1}\mathbf{D}\bar{\mathbf{P}}_i^{w/r}(\omega) = -\mathbf{A}_{wi}\bar{\mathbf{P}}_i^{w/r}(\omega) \quad (9)$$

where the minus means that the direction of wheel displacement is contrary to that of wheel-rail interaction force. The element a_{mn}^{wi} ($m=1, 2, \dots, N_{wi}; n=1, 2, \dots, N_{wi}$) of matrix \mathbf{A}_{wi} represents the displacement of the n -th wheel-sets when the unit harmonic loads with frequency of ω acts at the position of the m -th wheel-sets, and $a_{mn}^{wi} = a_{nm}^{wi}$.

Since each vehicle satisfies Eq. (9), for the train composed by N_v number of vehicles, the displacements of all wheel-sets can be expressed as a large vector equation:

$$\begin{Bmatrix} \bar{\mathbf{z}}_{w1}(\omega) \\ \bar{\mathbf{z}}_{w2}(\omega) \\ \vdots \\ \bar{\mathbf{z}}_{wN_v}(\omega) \end{Bmatrix} = - \begin{bmatrix} \mathbf{A}_{w1} & & \mathbf{0} & \\ & \mathbf{A}_{w2} & & \\ & & \ddots & \\ & & & \mathbf{A}_{wN_v} \end{bmatrix} \begin{Bmatrix} \bar{\mathbf{P}}_1^{w/r}(\omega) \\ \bar{\mathbf{P}}_2^{w/r}(\omega) \\ \vdots \\ \bar{\mathbf{P}}_{N_v}^{w/r}(\omega) \end{Bmatrix} \quad (10)$$

4.2 Track Model and Coupling with Vehicles

The track is regarded as a two-layer mass-spring-damper system, as shown in Figure 6. According to the definition of spatial angle frequency Ω , when the train runs at speed V , the wavelength of track irregularity is $\lambda=2\pi/\Omega$, and the circular frequency of irregularity is $\omega=2\pi f=2\pi V/\lambda$. So, the track irregularity at position x can be changed into that at position $x_{pil} = x_{pil}^0 + Vt$ of wheel-set, in which x_{pil}^0 is the initial coordinate of the il -th wheel-set, i.e.

$$\bar{z}_{til}(\omega_k) = \tilde{z}_r(\Omega_k) \cdot \exp(i \frac{\omega_k}{V} x_{pil}^0) \quad (11)$$

where $\bar{z}_{ril}(\omega_k)$ represents the amplitude of track irregularity with frequency ω_k at the position of the il -th wheel-set; $\tilde{z}_r(\Omega_k)$ is the amplitude of track irregularity with spatial frequency Ω_k . Thus, the track irregularity vector at the positions of all wheel-sets can be expressed as:

$$\begin{Bmatrix} \bar{\mathbf{z}}_{r1}(\omega_k) \\ \bar{\mathbf{z}}_{r2}(\omega_k) \\ \vdots \\ \bar{\mathbf{z}}_{rN_v}(\omega_k) \end{Bmatrix} = \tilde{z}_r(\Omega_k) \cdot \begin{Bmatrix} \mathbf{e}_1(\omega_k) \\ \mathbf{e}_2(\omega_k) \\ \vdots \\ \mathbf{e}_{N_v}(\omega_k) \end{Bmatrix} \quad (12)$$

in which $\bar{\mathbf{z}}_{ri}(\omega_k) = \{\bar{z}_{ri1}(\omega_k), \bar{z}_{ri2}(\omega_k), \dots, \bar{z}_{riN_{wi}}(\omega_k)\}^T$ represents the displacement vector of track irregularity at the positions of all wheel-sets for the i -th vehicle; the element of the last vector is $\mathbf{e}_i(\omega_k) = \{\exp(i\frac{\omega_k}{V}x_{pi1}^0), \exp(i\frac{\omega_k}{V}x_{pi2}^0), \dots, \exp(i\frac{\omega_k}{V}x_{piN_{wi}}^0)\}^T$.

The coupling of vehicle and track is accomplished by the wheel-rail contact relationship assumed by the Hertz contact theory, as shown in Figure 6. The relationship between wheel-rail interaction force and wheel-rail relative displacement can be expressed as:

$$\begin{Bmatrix} \bar{\mathbf{P}}_1^{w/r}(\omega_k) \\ \bar{\mathbf{P}}_2^{w/r}(\omega_k) \\ \vdots \\ \bar{\mathbf{P}}_{N_v}^{w/r}(\omega_k) \end{Bmatrix} = k_H \cdot \begin{Bmatrix} \bar{\mathbf{z}}_{w1}(\omega_k) \\ \bar{\mathbf{z}}_{w2}(\omega_k) \\ \vdots \\ \bar{\mathbf{z}}_{wN_v}(\omega_k) \end{Bmatrix} - \begin{Bmatrix} \bar{\mathbf{w}}_{r1}(\omega_k) \\ \bar{\mathbf{w}}_{r2}(\omega_k) \\ \vdots \\ \bar{\mathbf{w}}_{rN_v}(\omega_k) \end{Bmatrix} - \begin{Bmatrix} \bar{\mathbf{z}}_{r1}(\omega_k) \\ \bar{\mathbf{z}}_{r2}(\omega_k) \\ \vdots \\ \bar{\mathbf{z}}_{rN_v}(\omega_k) \end{Bmatrix} \quad (13)$$

in which k_H is the stiffness of Hertz contact; $\bar{\mathbf{w}}_{ri}(\omega_k) = \{\bar{w}_{ri1}(\omega_k), \bar{w}_{ri2}(\omega_k), \dots, \bar{w}_{riN_{wi}}(\omega_k)\}^T$, and $\bar{w}_{ril}(\omega_k)$ is the rail displacement at the position of the il -th wheel-set.

4.3 Rail Displacement Subjected to All Wheel-sets

When a single wheel-set load is applied to the rail, the force analysis and deformation of the rail is illustrated in Figure 7.

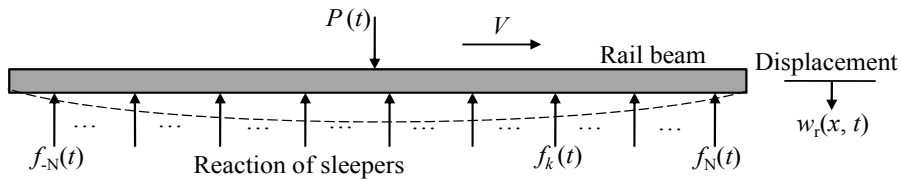


Figure 7: Force and deformation of rail under the action of a single wheel-set.

When $P(t)$ is a wheel-rail interaction force $\bar{P}^{w/r}(\omega_k)e^{i\omega_k t}$, the rail displacement induced by moving harmonic loading can be obtained as [10]:

$$\bar{w}_{ri}^{w/r}(x, \omega) = \frac{\bar{P}^{w/r}(\omega_k)}{V} \tilde{B}_r\left(\frac{\omega - \omega_k}{V}, \omega\right) \exp\left[-i(x - x_p^0)\frac{\omega - \omega_k}{V}\right] \quad (14)$$

in which $\tilde{B}_r(k_x, \omega) = 1/[E_r^* I k_x^4 - \bar{m}_r \omega^2]$ represents the rail displacement under unit impulse load in wavenumber-frequency domain; $E_r^* = E_r(1 + 2\xi_r i)$ is the complex elastic modulus taking

the internal damping of rail structure into account, where E_r is the real elastic modulus and ζ_r is the damping ratio of rail structure; I is the inertia moment of rail section; \bar{m}_r is the rail mass of unit length; x_p^0 is the initial position of load $P(t)$.

The rail displacement induced by supporting actions $\sum_{m=-N}^N f_m(t)\delta(x-x_m)$ of sleepers (see Figure 7) under single wheel-sets loading can be obtained by using the generalized Duhamel integral as [10]:

$$\bar{w}_{r2}(x, \omega) = \sum_{m=-N}^N \bar{f}_m(\omega) \bar{B}_r(x-x_m, \omega) \quad (15)$$

in which $\bar{B}_r(x, \omega) = [-e^{-\alpha|x|} - ie^{-i\alpha|x|}] / (4E^*I\alpha^3)$; $\alpha = \sqrt[4]{\bar{m}\omega^2 / E^*I}$; $\bar{f}_m(\omega)$ is the supporting force from the m -th sleeper to rail induced by moving load $P(t)$ with invariable position.

According to the arrangement of all wheel-sets of a train illustrated in Figure 6, the rail displacement induced by quasi-static axle loading and wheel-rail interaction force of running train can be respectively written as:

$$\bar{w}_r(x, \omega) = \frac{1}{V} \tilde{\bar{B}}_r\left(\frac{\omega}{V}, \omega\right) e^{-ix\frac{\omega}{V}} \left[\sum_{i=1}^{N_v} \sum_{l=1}^{N_{wm}} P_{0il} e^{ix_{pil}^0 \frac{\omega}{V}} \right] - \sum_{m=-N}^{+N} \bar{f}_m^{\text{final}}(\omega) \bar{B}_r(x-x_m, \omega) \quad (16)$$

$$\bar{w}_r(x, \omega) = \frac{1}{V} \tilde{\bar{B}}_r\left(\frac{\omega-\omega_k}{V}, \omega\right) e^{-ix\frac{\omega-\omega_k}{V}} \left[\sum_{i=1}^{N_v} \sum_{l=1}^{N_{wm}} \bar{P}_{il}^{w/r}(\omega_k) e^{ix_{pil}^0 \frac{\omega-\omega_k}{V}} \right] - \sum_{m=-N}^{+N} \bar{f}_m^{\text{final}}(\omega) \bar{B}_r(x-x_m, \omega) \quad (17)$$

in which $\sum_{m=-N}^N \bar{f}_m^{\text{final}}(\omega) \bar{B}_r(x-x_m, \omega)$ represents the supporting force from sleepers to rail under the action of all wheel-sets loading for a running train, ω is the vibration frequency of rail structure, and ω_k represents the loading frequency excited by running train.

4.4 Forces Transmitted to Ground Surface

According to the force analysis of sleepers, there is the following relationship:

$$\begin{aligned} \bar{\mathbf{f}} &= (k_{rs} + i\omega c_{rs})(\bar{\mathbf{w}}_s - \bar{\mathbf{w}}_r) \\ \bar{\mathbf{f}} - \bar{\mathbf{F}} &= m_s \omega^2 \bar{\mathbf{w}}_s \\ \bar{\mathbf{F}} &= (k_{sg} + i\omega c_{sg}) \bar{\mathbf{w}}_s \end{aligned} \quad (18)$$

where $\bar{\mathbf{f}} = \{\bar{f}_{-N}^{\text{final}}(\omega), \dots, \bar{f}_0^{\text{final}}(\omega), \dots, \bar{f}_N^{\text{final}}(\omega)\}^T$ is the column vector composed of supporting forces at the positions of all $2N+1$ sleepers induced by running train; $\bar{\mathbf{F}} = \{\bar{F}_{-N}(\omega), \dots, \bar{F}_0(\omega), \dots, \bar{F}_N(\omega)\}^T$ is the column vector consisting of interaction forces between $2N+1$ sleepers and subsoil; $\bar{\mathbf{w}}_r = \{\bar{w}_r(x_{-N}, \omega), \dots, \bar{w}_r(x_0, \omega), \dots, \bar{w}_r(x_N, \omega)\}^T$ can be expressed by Eqs. (16)-(17). $\bar{\mathbf{w}}_s = \{\bar{w}_s(x_{-N}, \omega), \dots, \bar{w}_s(x_0, \omega), \dots, \bar{w}_s(x_N, \omega)\}^T$ is the column vector composed of $2N+1$ sleeper displacements.

By combining Eqs. (10), (12), (13), and (18), the interaction force vector $\bar{\mathbf{F}}$ between sleepers and ground can be solved. When the force $\bar{\mathbf{F}}$ is applied to the 3-dimensional subsoil model, the ground vibrations can be obtained.

5 CASE STUDY

The China Star train composed of 1 locomotive + 4 passenger cars + 1 locomotive is taken as the train load, whose parameters can be found in reference [10]. The track parameters include: Rail: mass per unit length $\bar{m}_r=60$ kg/m, section stiffness $EI=6.63$ MN·m², damping ratio $\xi_r=0.01$; Sleeper: mass $m_s=250$ kg, spacing $d=0.55$ m; Ballast bed: mass $m_b=560$ kg; Spring-damper coefficients: $k_{rs}=78$ MN/m, $c_{rs}=50$ kN·s/m, $k_{sg}=65$ MN/m and $c_{sg}=90$ kN·s/m. The track irregularity is simulated by a single wavelength harmonic profile with the irregularity amplitude $\bar{z}_i(\Omega_k)$ equal to 0.2 mm.

Plotted in Figure 8 are the vertical ground acceleration histories of receiver points at 0 m, 5 m, 20 m, 30 m from the track, under the train speed of 200 km/h. The attenuation and propagation of ground vibration can be observed, and with the increase of distance, the relevance between the ground accelerations and the train excitation becomes less obvious.

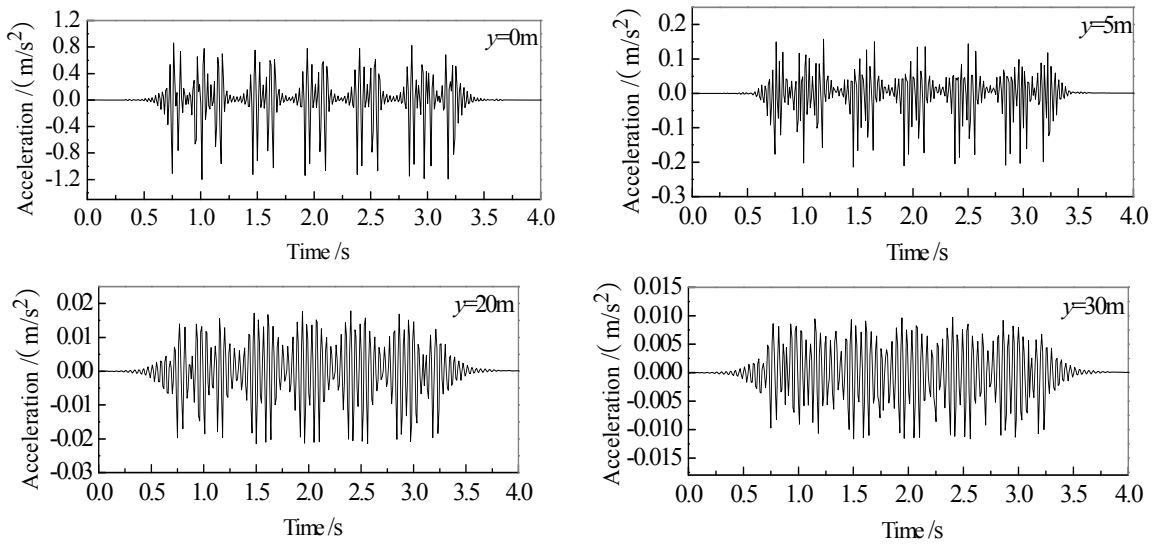


Figure 8: Acceleration histories of different receiver points on the ground.

The acceleration spectra for receiver point at 5 m and 20 m on the ground surface are shown in Figure 9. The high frequency components of ground vibration indicate that the dynamic responses excited by wheel-track irregularity cannot be neglected. Also, it can be found that with the increase of distance to the track, the higher frequency components of acceleration spectra become lesser, which can be explained by the dissipation of material damping and radiation damping in soil medium to higher frequency components in vibration energy.

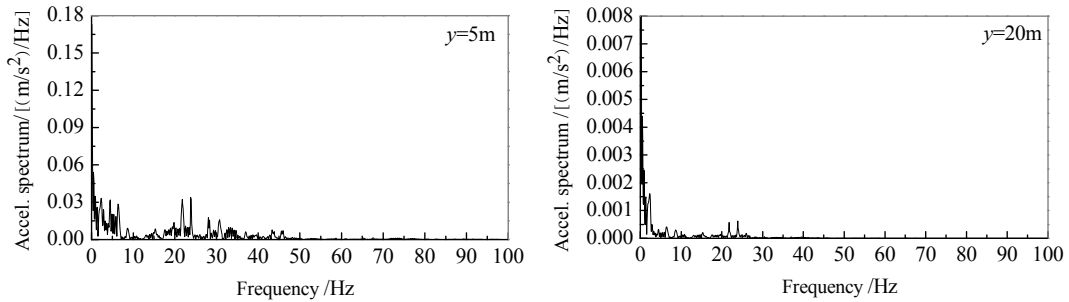


Figure 9: Acceleration spectra of different receiver points on the ground.

6 CONCLUSIONS

The paper develops a method based on a semi-analytical/numerical model to predict the ground vibrations induced by high-speed trains running on ground, in which the 3-dimensional finite element soil model with infinite element boundary and semi-analytical train-track dynamic interaction model are established. The analysed results show that:

(1) The ground vibration characteristics have a very close relationship with the soil properties and the speed of moving loads.

(2) The critical speed of soil vibration is close to the minimum speed of the Rayleigh's wave in the subsoil, and the resonant frequency is very close to the intersection frequency of the speed-lines of moving loads and the P-SV dispersion curves of the subsoil model.

(3) The dynamic responses excited by wheel-track irregularity cannot be neglected, which has big influence on the high frequency components of ground vibration.

(4) The dynamic responses excited by wheel-track irregularity cannot be neglected.

7 ACKNOWLEDGEMENTS

This study is sponsored by the National Natural Science Foundation of China (Grant No. 51108023), and the Fundamental Research Fund of Beijing Jiaotong University (2011JBM088).

REFERENCES

- [1] Madshus C., Kaynia A.M. High-speed railway lines on soft ground: dynamic behavior at critical train speed. *Journal of Sound and Vibration*, 231(3), 689–701, 2000.
- [2] Kaynia A.M., Madshus C., Harvik L., et al. Ground vibration from high-speed trains: prediction and countermeasure. *Journal of Geotechnical and Geoenvironmental Engineering, American Society of Civil Engineers*, 120 (6), 531-537, 2000.
- [3] Lombaert G., Degrande G. Ground-borne vibration due to static and dynamic axle loads of InterCity and high-speed trains. *Journal of Sound and Vibration*, 319(3-5), 1036-1066, 2009.
- [4] Sheng X., Jones C.J.C., Thompson D.J. A theoretical model for ground vibration from trains generated by vertical track irregularities. *Journal of Sound and Vibration*, 272, 937-965, 2004.
- [5] Yang Y.B. Train-induced wave propagation in layered soils using finite/infinite element simulation. *Soil Dynamics and Earthquake Engineering*, 23, 263-278, 2003.
- [6] Auersch L. The excitation of ground vibration by rail traffic: theory of vehicle-track-soil interaction and measurements of high-speed lines. *Journal of Sound and Vibration*, 284, 103-132, 2005.
- [7] Takemiya H. Simulation of track-ground vibrations due to a high-speed train: the case of X-2000 at Ledsgard. *Journal of Sound and Vibration*, 261, 503-526, 2003.
- [8] Masafumi K., Toshifumi M., Osamu Y., et al. Numerical simulation study of ground vibrations using forces from wheels of a running high-speed train. *Journal of Sound and Vibration*, 318, 830-849, 2008.
- [9] Lombaert G. *Development and experimental validation of a numerical model for the free vibrations induced by road traffic*. Belgium, Leuven University, 2001.
- [10] Cao Y.M. *Theoretical and Experimental Study on Train-induced Vibrations of Free Field and Buildings*. Beijing, Beijing Jiaotong University, 2006.